Efficacy of absorption of laser energy in the "Sokol" facility

Yu. A Zysin, I. A. Abramov, V. V. Volenko, N. P. Voloshin, A. I. Zuev, A. F. Ivanov, V. A. Lykov, L. A. Myalitsin, L. A. Osadchuk, and A. I. Saukov

(Submitted 26 April 1982)
Zh. Eksp. Teor. Fiz. **83**, 1346–1357 (October 1982)

Results are presented of an investigation of the absorption of laser energy by glass-shell microspheres. The experiments were performed with the high-power "Sokol" facility at laser energy flux densities $q \approx 0.3$–2×10^{14} W/cm^2 at the target. A numerical analysis of the efficacy of laser-energy absorption, based on the classical inverse-bremsstrahlung mechanism, is carried out with the aim of identifying the major absorption mechanism. Allowance is made for the refraction of the laser radiation in the "corona" and for the "steepening" of the density profile. The magnitude of the resonance absorption is estimated. The measured absorption efficacy and absorption coefficient agree well with the calculation results as well as with the results of experiments performed with the "Cyclops Laser" facility in the same flux-density range. The parameters of the fast-ion "jets" registered in the experiments with the "Sokol" facility are close to those measurements with the "Kal'mar" facility at the same laser-energy flux densities.

PACS numbers: 42.60.Kg, 52.25.Ps

INTRODUCTION

A run of experiments on the irradiation of spherical gas-filled glass-shell targets have by now been performed with the high-power "Sokol" laser facility.[1] The experiments included measurements of the energy and of the gasdynamic parameters of a laser plasma and proceeded along two lines.

The first comprised investigation of the efficiency and of the absorption coefficient, identification of the main mechanism whereby the laser energy is absorbed, measurement of the fast-particle parameters, as well as the development of the physical models necessary to explain the experimental results and the predict the interaction process at higher laser-energy flux densities.

The second comprised investigation of the gasdynamic processes of expansion and contraction of the targets, of the heating of the DT gas, and of generation of neutrons. A characteristic feature of "Sokol" experimental conditions is the adiabatic regime of the DT-gas compression, wherein it is possible to obtain large values of volume compression $\delta \approx 10^4$ and densities $\rho_{DT} \gtrsim 10$ g/cm^3. This regime, in contrast to the regime with a "burn-through" shell,[2,3] is less stable gasdynamically, but is the only one capable of yielding appreciable gains in laser-driven fusion experiments.[4]

1. ANALYSIS OF THE RESULTS OF MEASUREMENTS OF THE ABSORPTION EFFICIENCY. ROLE OF REFRACTION AND OF THE EFFECT OF "STEEPENING" OF THE DENSITY PROFILE IN THE ABSORPTION OF LASER RADIATION

Measurements of the efficiency $\varepsilon_{abs} = E_{abs}/E_0^k$ (E_{abs} is the laser energy absorbed by the target, E_0^k is the energy of the laser pulse in the target region) and of the laser-energy absorption coefficient $K_{abs} = \varepsilon_{abs}/f_g$ ($f_g = 1 - \exp[-(R_{cr}^{max}/\rho_e)^2]$, R_{cr}^{max} is the maximum radius of the "corona" region with critical electron density) in experiments with the "Sokol" facility were performed with the aid of the "shock-wave" and "corona" diagnostic procedures. The laser energy E_{abs} absorbed by the target was measured by the "shock-wave" method described in Ref. 1, while the dynamics of the behavior of the corona region with critical density n_e^{cr} was registered by a "corona" method similar to that in Refs. 5–8.

A typical result of measurements in the flux-density region $q \approx (0.3$–$2) \times 10^{14}$ W/cm^2 is low absorption efficiency $\varepsilon_{abs} \approx (0.1$–$0.25)$. The values obtained, as will be shown below, are in fair agreement with the results of experiment with the "Cyclops Laser" (Refs. 9 and 10) obtained at the same light fluxes.

To explain the measured values of ε_{abs}, and also to identify the main absorption mechanism, we analyze in the present section the experimental results on the laser-energy absorption efficiency. Since the optical thickness of the laser plasma, and consequently also the absorption efficiency, depends substantially on the target-irradiation method and on the shape of the plasma-density profile in the corona,[11,12] the analysis was carried out with accounts taken of the refraction of the laser radiation in the "corona" of spherical targets[13] and of the density-profile "steepening" due to the electromagnetic pressure of the laser radiation.[14–17] We analyzed an experiment in which the laser-pulse energy $E_L \approx 133$ J at the output of the facility, the laser-pulse energy $E_0^c \approx 81$ J in the chamber, the laser-pulse duration $\tau_p \approx (0.8 \pm 0.1)$ nsec, the focal-spot diameter at the e level is $2\rho_e \approx 150\ \mu$m, $q \approx 1.5 \times 10^{14}$ W/cm^2, the target diameter is $2R_t \approx 132.6\ \mu$m, the average shell thickness $\Delta R = (\Delta R_{max} + \Delta R_{min})/2 \approx 2.8\ \mu$m, the target mass is $M_0 \approx 390$ ng, and the pressure of the air surrounding the target is $P_0 \approx 3.45$ Torr. The laser energy absorbed by the target in this case is $E_{abs} \approx 13.6$ J, $\Delta E_{abs}/E_{abs} \approx \pm 25\%$, the calculated value of the x-ray energy is $E_r \approx (0.1$–$0.2) E_{abs}$, $2R_{cr}^{max} \approx 169\ \mu$m, $R_{cr}^{max}/R_t \approx 1.27$, $\delta R_{cr} \approx \pm 10\ \mu$m, and $f_g \approx 0.75$ (see Fig. 1).

At normal incidence of the laser radiation on the target surface the absorption efficiency ε_{abs}, assuming a classical inverse-bremsstrahlung mechanism,[18] is given by

 0038-5646/82/100773-07$04.00

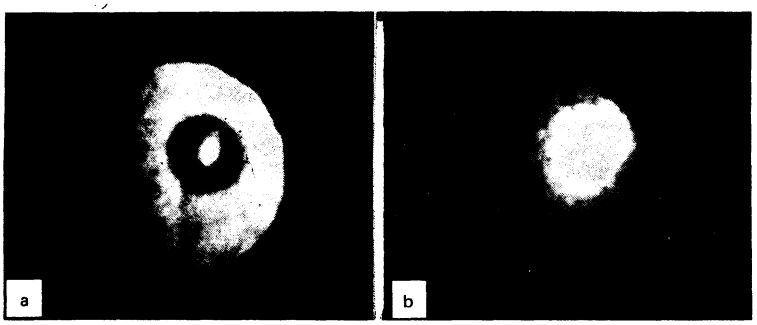

FIG. 1. a) Shadow image of the target prior to the start; b) integral image of the target in light of the second harmonic.

$$\varepsilon_{abs}=\frac{E_{abs}}{E_0^{\kappa}}=\left[1-\exp\left(2\int_{\infty}^{R_{cr}}K_{\omega_0}dr\right)\right]; \quad (1)$$

$$K_{\omega_0}=\frac{\nu_{ei}}{c}\frac{n_e}{n_e^{cr}}\left(1-\frac{n_e}{n_e^{cr}}\right)^{-1/2},\ \nu_{ei}=\frac{4}{3}\left(\frac{2\pi}{m_e}\right)^{1/2}\frac{\langle Z^2\rangle e^4 n_i}{T_e^{3/2}}\Lambda_{ei}; \quad (2)$$

n_e^{cr} is the electron critical density, with $n_e^{cr}\approx 10^{21}$ cm^{-3} for λ_0 1.06 μm; m_e and e are the electron mass and charge; c is the speed of light. According to the results of a gasdynamic calculation in accord with the three-temperature program "ERA," carried out for an absorbed energy $E_{abs}\approx 13.6$ J, the electron temperature in the region $n_e\leqslant n_e^{cr}$ is $T_e^{cr}\approx 0.6$ keV; the maximum radius of the corona region with $n_e=n_e^{r}$ is $R_{cr}^{max}\simeq 88$ μm; in the region $n_e\leqslant n_e^{cr}$ the electron density is $n_e(r)=n_e^{cr}(R_{cr}/r)^3$. The Coulomb logarithm is $\Lambda_{ei}\approx 6$; $\langle Z^2\rangle/\langle Z\rangle\cong 10$ and then the efficiency is $\varepsilon_{abs}\approx 0.96$. This is not a realistic result since normal incidence is known not to be achieved in the "Sokol" experiments; the focal spot is $2\rho_e\approx 150\,\mu$m $\approx 2R_{cr}^{max}$. Allowance for the refraction of the laser radiation in the corona of the spherical targets in the analysis should therefore lower the calculated efficiency ε_{abs}.

We consider now the efficiency ε_{abs} with allowance for the refraction of the laser radiation in the geometric-optics approximation.[13] It is assumed here that a plane laser-radiation front is incident on the target. The trajectory of the laser beam incident on the target with impact parameter ρ is described in polar coordinates (r, φ) by the expression

$$\varphi(r)=\varphi(\infty)+\int_r^{\infty}\frac{\rho\,dr}{r[n^2(r)r^2-\rho^2]^{1/2}},\quad n(r)=\left(1-\frac{n_e(r)}{n_e^{cr}}\right)^{1/2}. \quad (3)$$

The optical thickness of the laser plasma along the beam trajectory with impact parameter ρ to the turning point $r_0(n^2(r)r^2-\rho^2|_{r_0}=0)$ is defined as

$$\tau(\rho)=\int_{r_0}^{\infty}K_{\omega_0}dS=\int_{r_0}^{\infty}K_{\omega_0}(r)\frac{n(r)\,r\,dr}{[n^2(r)\,r^2-\rho^2]^{1/2}} \quad (4)$$

$$=\tau(\xi)=R_{cr}^{max}\int_{r_0/R_{cr}^{max}}^{\infty}K_{\omega_0}(\eta)\frac{n(\eta)\,\eta\,d\eta}{[n^2(\eta)\,\eta^2-\xi^2]^{1/2}},$$

where

$$\eta=r/R_{cr}^{max},\quad \xi=\rho/R_{cr}^{max},\quad \tau(\xi)=\tau_c J(\xi),$$

$$\tau_c=R_{cr}^{max}\nu_{ei}/c|_{n_e=n_e^{cr}}.$$

The absorption efficiency is $\varepsilon_{abs}=1-R$, where R is the reflection coefficient, defined for a Gaussian distribution of the energy in the focal spot as

$$R=\frac{2}{\mu^2}\int_0^{\infty}\xi\,d\xi\exp\left[-\left(\frac{\xi^2}{\mu^2}+2\tau(\xi)\right)\right],\quad \mu=\frac{\rho_e}{R_{cr}^{max}}. \quad (5)$$

For a cubic profile of the electron density, the problem (3)–(5) was solved numerically. Figure 2 shows a $J(\xi)$ plot that describes the behavior of the optical thickness $\tau(\xi)$ as a function of the impact parameter ξ. Figure 3 shows plots of the reflection coefficient against the optical thickness τ_c for a number of values of $\mu=\rho_e/R_{cr}^{max}$. At the parameters of the corona of the type considered we have $\tau_c\approx 3.3$ and $\mu\approx 0.9$; consequently, the calculated values are $R\approx 0.35$ and $\varepsilon_{abs}\approx 0.65$; this likewise does not explain the experimental absorption efficiency $\varepsilon_{abs}\approx(0.17\pm 0.06)$. To obtain a reflection coefficient $R\approx 0.8$ it is a necessary to either increase the calculated temperature T_e^{cr} by 2.5 times or incur an error by a factor of 2 in the radius of the focal spot.

Calculations performed under various assumptions show that the temperatures can be calculated with accuracy not worse than 20%. On the other hand, the accuracy of the focal spot is $\approx 10\%$. As a result, the reflection coefficient, when account is taken of the possible errors in T_e^{cr} and ρ_e, should be less than $R\lesssim 0.45$, likewise contradicting the measured value $R\approx(0.83\pm 0.06)$. This contradiction is not eliminated by the possible errors in the aiming $(x;\ y)$ and focus-

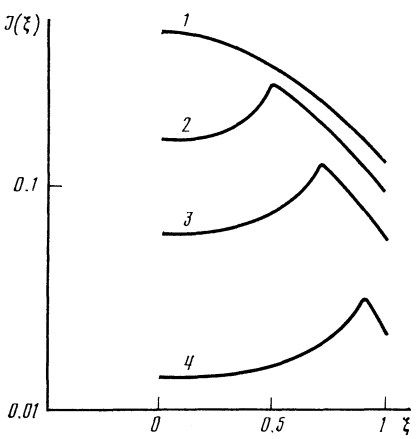

FIG. 2. The function $J(\xi)$ which characterizes the change of the optical thickness $\tau(\xi)$ with changing impact parameter ξ: 1—$\rho_- = \rho_{cr}$; 2—$\rho_- = 0.75\rho_{cr}$; 3—$\rho_- = 0.5\rho_{cr}$; 4—$\rho_- = 0.25\rho_{cr}$.

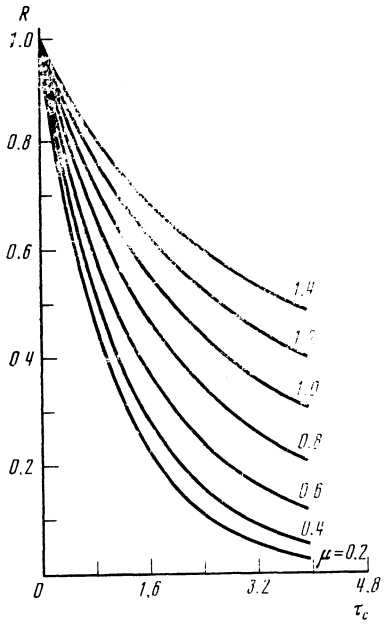

FIG. 3. Dependence of the reflection coefficient on the optical thickness τ_c for a number of values of $\mu = \rho_e / R_{cr}^{max}$.

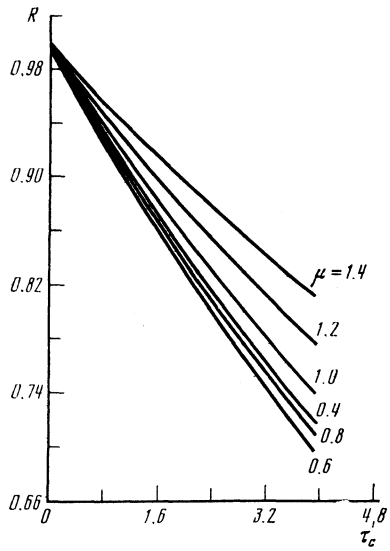

FIG. 4. Dependence of the reflection coefficient on the optical thickness τ_c for a number of values of $\mu = \rho_e / R_{cr}^{max}$; $\rho_- = 0.4\rho_{cr}$.

ing (z) of the laser beams on the spherical targets. Thus, the accuracy of the aiming along the x and y axes ensured by the adjustment system of the "Sokol" facility is $\lesssim 10\,\mu$m (Ref. 1), while the inaccuracy of setting the focal plane of the lens on the z axis ($\approx 50\,\mu$m) increases the size of the focal spot by not more than $\sim(10\text{–}20\,\mu$m).

In the foregoing calculations we did not take into account one of the effects that is typical of the corona at fluxes $q \gtrsim 10^{14}$ W/cm^2, which may explain the experimentally observed absorption efficiency. We have in mind the increase of the slope of the density profile as a result of electromagnetic pressure of the laser radiation in the region of a corona with critical density. This effect was observed in experiments[17] and extensively discussed theoretically.[14–16] The gist of the density-profile steepening reduced to the following. The electric field of the laser radiation, which increases near the critical region, leads to an abrupt change in the density profile near ρ_{cr} at a distance equal to several Debye lengths, i.e., practically to a density jump from ρ_+ to ρ_-.

No account is taken in the "ERA" program of effects connected with the electromagnetic pressure of the laser radiation. The calculations of the trajectory (3), of the optical thickness (4), and of the reflection coefficient (5) of the laser radiation were therefore performed on a model density profile

$$\rho(r) = \begin{cases} \infty; & r \leqslant R_{cr}^{max} \\ \rho_-(R_{cr}^{max}/r)^3; & r > R_{cr}^{max}, \end{cases} \tag{6}$$

i.e., it was assumed that at $r = R_{cr}^{max}$ there is located a mirror to which is adjacent the corona that starts with a density $\rho = \rho_-$ whose dependence on the radius is the same as in the calculations without allowance for the laser-radiation pressure.

The value of the jump of ρ_-/ρ_{cr} for the considered experiment was estimated on the basis of the results of Refs. 14–17. It is shown in Ref. 16 that

$$\frac{|\rho_- - \rho_{cr}|}{\rho_{cr}} \sim \left(\frac{P_L}{P_T}\right)^{1/2}, \tag{7}$$

where $P_L = q/c$ is the laser radiation pressure and $P_T = n_e^{cr} T_e^{cr}$ is the thermal pressure in the ρ_{cr} region. A density jump with $\rho_+ \approx 1.1\rho_{cr}$ and $\rho_- \approx 0.3\rho_{cr}$ and with a transition region $l \approx 1.6\,\mu$m was observed with the "Argus" facility[17] in experiments on spherical irradiation of glass shell targets. In accord with these results, and also using the $T_e \sim q^{3/5}$ dependence,[19] we obtain for the experiment considered $\rho_- \approx 0.4\rho_{cr}$.

The results of the numerical calculations carried out with the density profile (6) and with the steepening $\rho_- \approx 0.4\rho_{cr}$ are shown in Fig. 2 and Fig. 4. For the experiment considered $\tau_c \approx 3.3$, $\mu \approx 0.9$, and the reflection coefficient is $R \approx 0.78$, in agreement with the experiment data.

Thus, calculations of the efficiency of laser-energy absorption with allowance for refraction and of the effect of steepening of the density profile under the influence of the laser-radiation pressure are in good agreement with the experimental results. The density jump leads to a decrease of the absorption due to the inverse bremsstrahlung mechanism, to a decrease in the role of the refraction (see Fig. 2), and to an increase in the role of resonant absorption,[19,20] which amounts at fluxes $q > 10^{15}$ W/cm^2 to an appreciable fraction of the absorbed laser energy.

2. ESTIMATE OF THE EFFICIENCY OF RESONANT ABSORPTION. RESULTS ON REGISTRATION OF FAST-ION "JETS"

The resonant absorption coefficient for radiation with a p-polarization fraction f_r, incident at an angle θ on a plasma layer with an inhomogeneity scale $L = (\partial \ln\rho/\partial r)^{-1}|_{R_{cr}}$, is equal to [23]

$$K_r(\theta) = {}^1/_4 \Phi^2(\tau) f_r, \tag{8}$$

where $\Phi(\tau)$ is the resonance function.

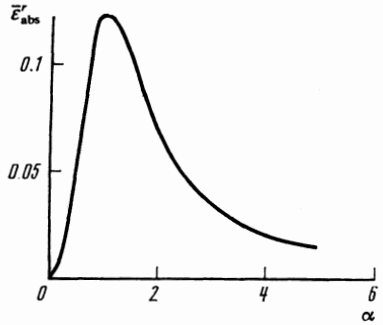

FIG. 5. Dependence of the resonant absorption efficiency $\bar{\varepsilon}^r_{abs}$ on the parameter $\alpha = (2\pi L/\lambda_0)^{1/3}\rho_e/R_{cr}^{max}$.

For a plane linearly polarized light wave with a Gaussian distribution, incident on a sphere of radius R_{cr}^{max}, the efficiency of the resonant absorption is

$$\bar{\varepsilon}^r_{abs} = \int_0^{(R_{cr}^{max}/\rho_e)^3} dx e^{-x} \bar{f}_r \frac{\Phi^2(\tau)}{4}; \quad \tau = x^{1/2}\left(\frac{2\pi L}{\lambda_0}\right)^{1/3}\frac{\rho_e}{R_{cr}^{max}}. \tag{9}$$

Figure 5 shows the dependence of $\bar{\varepsilon}^r_{abs}$ on the parameter $\alpha = (2\pi L/\lambda_0)^{1/3}\rho_e/R_{cr}^{max}$ for $\bar{f}_r = 0.5$. At $\rho_e/R_{cr}^{max} \approx 0.9$ and $L \approx (1-2)$ μm the efficiency is $\varepsilon^r_{abs} \approx 0.06$, amounting to $\approx 30\%$ of the experimental value $\varepsilon_{abs} \approx (0.17 \pm 0.06)$.

It is difficult to identify the mechanism whereby the energy of the plasma Langmuir oscillations are dissipated under the conditions of the experiments in question. If the main dissipation mechanism constitutes electron-ion collisons, this leads to an effective increase of the classical (thermal) absorption. However, collisionless dissipation mechanisms are also possible and can lead to the appearance of fast laser-plasma particles.[21-23] In this case the resonant part of the absorbed energy may also not enter into the energy of the shock wave propagating in the air surrounding the target, if the mean free paths of the fast particles in the surrounding air exceed $\sim$(3–5) mm, as is possible for electrons with energies $\gtrsim$(3–5) keV and for ions with energies $\gtrsim 20$ keV.

In the case of production of fast electrons in a continuous x-ray spectrum, the high-energy at "tails" must increase like[24,25]

$$I(h\nu)\,[\text{J/keV}] \approx 2\cdot 10^{-6}\varepsilon_{abs}{}^r E_0^k \exp(-h\nu/\varepsilon_e^f)\frac{\langle Z^2\rangle}{\langle Z\rangle}, \tag{10}$$

where $\varepsilon_e^f \approx \alpha_e T_e$ is the energy of the fast electrons, $\alpha_e \approx (4\text{–}10)$, $\langle Z^2\rangle$, and $\langle Z\rangle$ are the mean values of the square of the charge and of the charge of the nuclear matter in which the fast electrons slow down. Similar high-energy tails were rgistered in the x-ray spectrum in experiments performed both at high flux densities $q \approx 10^{15}$–10^{17} W/cm^2 (Ref. 25), and at flux densities $q \approx 10^{14}$ W/cm^2 that are typical of the "Sokol" facility.[9,10,26] These tails predominate in the spectrum at x-ray photon energies $(h\nu) \gtrsim 10$ keV. The appearance of high-energy tails at fluxes $q \approx 10^{14}$ W/cm^2 confirms the conclusion that the role of the resonant absorption increases under conditions when the density profile becomes steeper.

Resonant interaction may cause also the appearance of fast ions having energies $\sim$(100–500) keV and carrying $\approx$(10–50)% of the laser energy absorbed by the target.[21,22] Production of fast ions with the parameters indicated were observed in experiments.[27,32]

Measurements of the continuous x-ray spectrum in experiments on the "Sokol" facility show the presence of high-energy tails with $(h\nu) \gtrsim 10$ keV at $q \gtrsim 10^{14}$ W/cm^2 (Ref. 33). At fluxes $q \gtrsim 10^{14}$ W/cm^2, "jets" of fast ions were quite regularly observed in the experiments with the "Sokol" facility (see Fig. 6). The parameters of the registered fast-ion jets are listed in Table I (the following notation is used: Q is the specific energy of the cylindrical shock wave, N_i^f is the number of fast ions in the jet, N_{SiO_2} is the number of SiO_2 molecules in the target, ε_i^f is the lower limit of the fast-ion energy, E_i^f is the total energy of the fast ions in the jet). The procedure used for the estimates is similar to that in Ref. 29. Although the detailed mechanism whereby the fast-ion jets are produced is not fully clear and, in principle, one cannot exclude the possiblity of a different explanation, we adhere to the interpretation proposed in Refs. 29 and 31.

It can be seen that the parameters of the fast-ion jets registered in the experiments with the "Sokol" facility are close to those measured at the Lebedev Physics Institute with the "Kal'mar" facility[29,31]; the reason is that the experimental conditions were close.

The experimental values of the jet parameters agree in order of magnitude with estimates based on an analysis of the resonant interaction (see Fig. 5 and Ref. 29). The fraction of the absorbed energy carried away by the fast ions in the jet amounts to 10%, in agreement with the estimates of the resonant-absorption efficiency.

The jetlike emission of the fast ions from the target is due, according to Refs. 29 and 31, to the predominance of resonant interaction in some region of the corona, in which the polarization composition of the laser radiation is closer to optimal. A confirmation of this may be the fact that in the

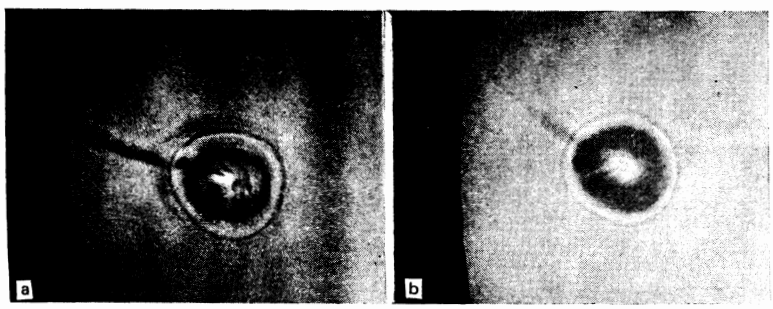

FIG. 6. Typical shadow photographs of fast-ion jets; a – $q \approx 1.2 \cdot 10^{14}$ W/cm^2; b – $q \approx 1.9 \cdot 10^{14}$ W/cm^2.

Table I:

	q, W/cm^2	Q, J/cm	N_i^f	N_{SiO_2}	B_i^f/N_{SiO}	i^f, keV	E_i^f, J	E_{abs}, J	$(E_i^f/E_{abs})\cdot 100\%$
«Sokol»	$1.2\cdot10^{14}$	0.14	$4\cdot10^{13}$	$3\cdot10^{15}$	0.01	150	1	8	12%
«Sokol»	$1.9\cdot10^{14}$	0.24	$8\cdot10^{13}$	$3.6\cdot10^{15}$	0.02	100	1.5	11.7	12%
«Kal'mar»	10^{14}	0.05	$2\cdot10^{13}$	$2\cdot10^{15}$	0.01	500	1.5	(7.5–15)	(5–10) %

different experiments with the "Sokol" facility the directions of the jets emitted from the target were close.

Fast-jet ions with the parameters listed in the table were observed in the "Sokol" facility under the experimental conditions only at fluxes $q \gtrsim 10^{14}$ W/cm^2. This indicates that the role of the resonant interaction increases at fluxes $q \gtrsim 10^{14}$ W/cm^2, and is due to turn to a manifestation of the steepening of the density profile under the influence of the electromagnetic pressure of the laser radiation at flux densities $q \gtrsim 10^{14}$ W/cm^2.

3. DEPENDENCE OF R_{cr}^{max}/R_t AND OF THE ABSORPTION COEFFICIENT K_{abs} ON THE FLUX DENSITY q OF THE LASER ENERGY INCIDENT ON THE TARGET

It was shown with the aid of numerical calculations (see Fig. 7) that if the instant t_m of the maximum compression of the shell targets takes place at the "end" of the laser pulse, $R_{cr}^{(t)}$ changes little during the time $(t - t_0) \approx (-0.5\text{–}0.5)$ nsec, and the maximum value of R_{cr}^{max} is reached at the instant of time $t \approx t_0$ when the $(2\omega_0)$ radiation is generated with maximum intensity. Measurements performed by the "corona" method in the slit regime of time scanning the target image in $(2\omega_0)$ light in experiments with $t_m \geqslant \tau_p^{bas}$ (τ_p^{bas} is the duration of the laser pulse at the base) confirmed this picture. Accordingly, the smearing of R_{cr}^{max} on account of the motion of the n_e^{cr} region is negligible. Inasmuch as in this case the influence of the refraction of the second-harmonic rays in the target corona on the measured quantity $R_{2\omega_0}^{max}$ lies within the limits of the resolution (a calculation performed in the present study has shown that the measured size of the image is $R_{2\omega_0}^{meas} \approx 0.96 R_{cr}$), it follows that the measured size of the integral image of the target in $(2\omega_0)$ light is $R_{2\omega_0}^{max} \approx R_{cr}^{max}$.

Results of mesurements of the R_{cr}^{max}/R_t dependence for the case $t_m \geqslant \tau_p^{bas}$ at an incident laser energy flux density $q \approx (0.2\text{–}2)\times 10^{14}$ W/cm^2 are shown in Fig. 8. The experimental results are well approximated by their relation $R_{cr}^{max}/R_t \sim q^{1/8}$.

Gasdynamic calculations with the three-temperature "ERA" program are in agreement with the experimental results on the maximum value of the radius of the corona region with the critical electron density. Thus, in particular, for the experiment considered, calculation at the measured absorbed energy $E_{abs} \approx 13.6$ J yields $R_{cr}^{max} \approx 88\ \mu$m (see Fig. 7), in good agreement with the measured value $R_{cr}^{max} = (85 \pm 10)\ \mu$m.

Figures 9 and 10 show the measured laser enregy absorbed by the target and normalized to the geometric interaction factor $f_g = 1 - \exp[-(R_{cr}^{max}/\rho_e)^2]$, and of the laser-radiation absorption coefficient, defined as $K_{abs} = E_{abs}/E_0^k f_g$, as functions of the flux density q of the energy incident on the target. The dependence of E_{abs}/f_g on q is well approximated by $E_{abs}/f_g \sim q^{0.44}$, and dependence of K_{abs} on q by $K_{abs} \sim q^{0.5}$ in the flux range q $(0.2\text{–}2)\times 10^{14}$ W/cm^2.

The absorbed energy normalized to f_g is $E_{abs}/f_g = K_{abs}(q) q \times 4\pi\rho_e^2\tau_p$. Since $K_{abs} \sim q^{-0.5}$, we have $E_{abs}/f_g \sim E_0^{k\,0.5}\tau_p^{0.5}$, at the same values of ρ_e and R_t, i.e., at the same incident energies E_0^k and at the same ρ_e and R_t the laser energy absorbed by the target is larger if the pulse duration is longer. The laser-energy flux absorbed by the target, defined as $q_{abs} = qK_{abs}(q)$, is $q_{abs} \sim q^{0.5}$ according to Fig. 10.

Figure 10 shows also the experimental results obtained with the "Cyclops Laesr" at fluxes $q \approx (0.1\text{–}2)\times 10^{14}$ W/cm^2 (Refs. 9 and 10). The results obtained in the present study are in fair agreement with the results of Refs. 9 and 10 in the considered range of flux densities. It must be noted here that, just as in the present study, the absorption coefficient measured with the "Cyclops Laser" facility agree with results of calculations performed by the LASNEX program only when account is taken of the steepening of the density profile un-

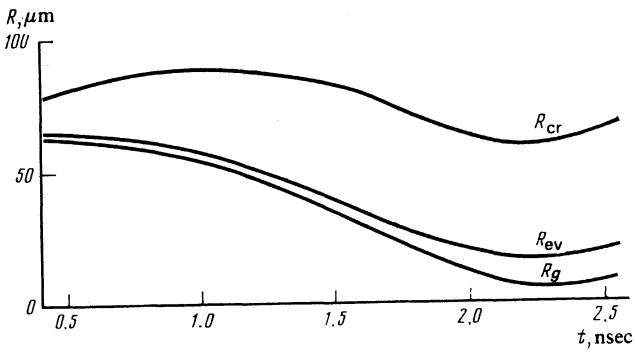

FIG. 7. (R-t) diagrams of the corona region with critical density R_{cr}, of the evaporation limit R_{ev}, of the internal gas-glass interface R_g, all obtained by calculation with the "ERA" program for the experiment considered.

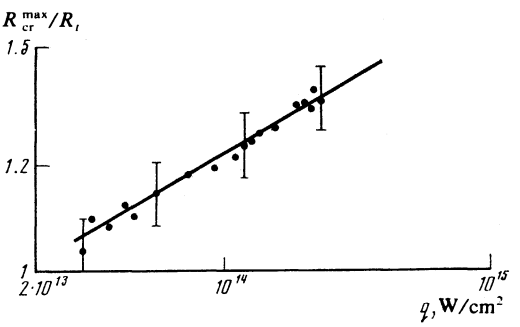

FIG. 8. Dependence of R_{cr}^{max}/R_t on the flux density q for the case $t_m \geqslant \tau_p^{bas}$.

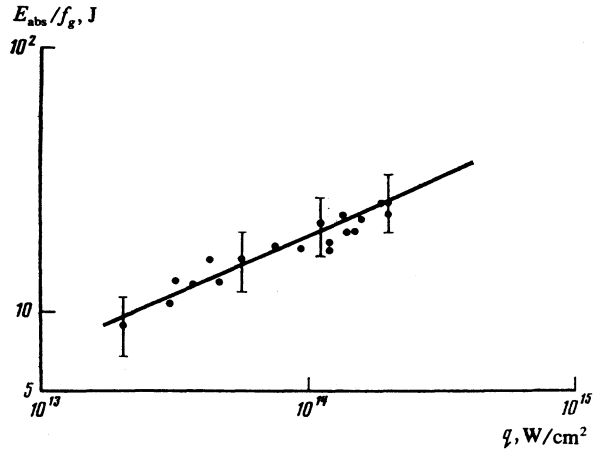

FIG. 9. Dependence of the absorbed energy E_{abs}/f_g on the flux density q.

der the influence of the laser-radiation pressure.[10] It must also be noted that the true laser-energy absorption coefficient can differ from the measured value more readily on the high side than on the low, since uncontrollable experimental conditions can lead only to a decrease of the energy incident on the target.

The measured dependences of the laser energy E_{abs} absorbed by the target on the target radius at a fixed value of the incident energy E_0^{k*} are shown in Fig. 11. The parameters are the following: $E_0^{k*} \approx 100$ J; $\tau_P \approx 0.8 \times 10^{-9}$ sec; $2\rho_e \approx 150\ \mu$m; $q_* \approx 2 \times 10^{14}$ W/cm^2; the absorption coefficient $K_{abs}(q)$ and R_{cr}^{max}/R_t at the given flux q_* are given by $K_{abs}(q_*) \approx 0.18$ (see Fig. 10) and $R_{cr}^{max}/R_t \approx 1.34$ (see Fig. 8). The same Fig. 11 shows the dependence of the absorbed energy $E_{abs}(R_t; q_*)$ on the value of R_t obtained under the assumption that the absorption coefficient $K_{abs}(q_*)$ is independent of the target radius R_t: $E_{abs}(R_t; q_*) = K_{abs}(q_*) E_0^{k*} f_g(R_t; q_*)$. The results of the numerical calculations of the laser-energy absorbed by the target, based on the model (3)–(7), are also given in Fig. 11. It is seen that the experimental results agree within the lmits of error with calculations based on the classical inverse-bremsstrahlung mechanism, when account is taken of refraction and of the steepening of the density profile.

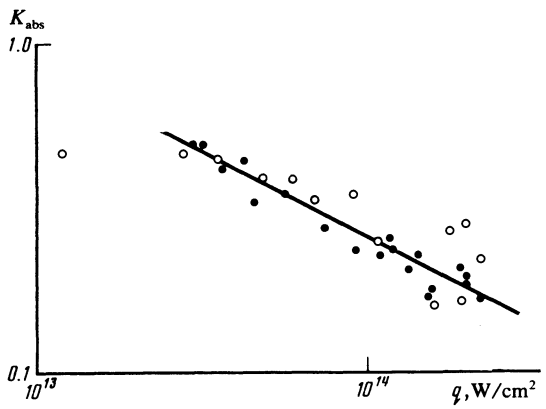

FIG. 10. Dependence of the absorption coefficient $K_{abs} = E_{abs}/E_0^k f_g$ on the flux density q; light circles—values from Refs. 9 and 10.

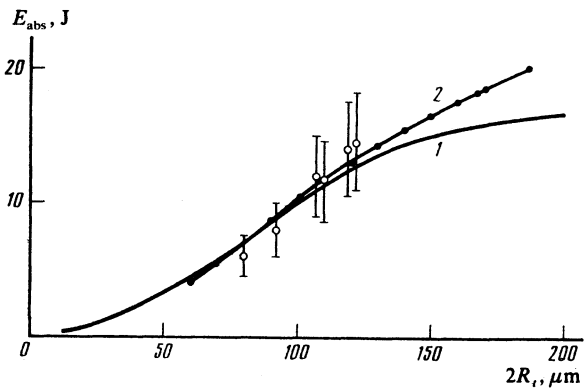

FIG. 11. Dependence of the laser energy E_{abs} absorbed by the target on the target radius R_t at a fixed value of the incident laser energy: 1) $E_{abs}(R_t; q_*)$; 2) numerial calculation.

It can also be seen from Fig. 11 that the values of E_{abs} calculated on the basis of the model (3)–(7) and the results for $E_{abs}(R_t; q_*)$ are close to one another in the radius regions $2R_t \approx (50–130)\ \mu$m. The reason is that in this target-radius region the absorption coefficient K_{abs} does not depend strongly on the target size. This in turn is due to the specific dependence of the optical thickness $\tau(\xi)$ of the laser plasma on the impact parameters $\xi = \rho/R_{cr}^{max}$ (see Fig. 2) under conditions when the density profile is steepened. This is a rather important fact, for in this case the asymmetry of the illumination of the spherical targets in multichannel laser systems, which was calculated in Refs. 34–36, can apparently be treated as the asymmetry of the laser-energy absorption.

CONCLUSION

The measurements and the analysis of the efficiency of laser-energy absorption in the experiments with the "Sokol" facility have shwon that the principal absorption mechanism in the flux range $q \approx (0.3–2) \times 10^{14}$ W/cm^2 is the classical inverse-bremsstrahlung mechanism. A substantial role in the absorption of the laser energy is played by the steepening of the density profile, which is typical of laser experiments at fluxes $q \geqslant 10^{14}$ W/cm^2. When steepening occurs, the absorption due to the inverse-bremsstrahlung mechanism decreases, as does a role of refraction, and the role of resonant absorption increases. Estimates show that at $q \approx 1.5 \times 10^{14}$ W/cm^2, $L \cong 1–2\ \mu$m, and $R_{cr}^{max} \approx \rho_e$ the efficiency of resonant absorption can amount to $\bar{\varepsilon}_{abs}^r \approx 0.06 \approx 0.3 \varepsilon_{abs}$.

According to contemporary physical concepts, resonant interaction can lead to the appearance of fast electrons, leading in turn to the appearance of high-energy tails in the region $h\nu \gtrsim 10$ keV of the x-ray spectrum and to the appearance of jets of fast ions. Results on registration of jets of fast ions in the experiments with the "Sokol" facility confirm the conclusion that the resonant absorption increases when steepening takes place at fluxes $q \gtrsim 10^{14}$ W/cm^2.

The measurements of the dependences of R_{cr}^{max}/R_t and K_{abs} on the flux density q and of E_{abs} on R_t at constant E_0^k show that the experimental results agree well both with the calculation results and with the results of experiments performed with the "Cyclops Laser" facility in the same range of laser-energy flux densities.

[1]I. A. Abramov, V. V. Volenko, N. P. Voloshin, *et al.*, Zh. Eksp. Teor. Fiz. **83**, 988 (1982) [Sov. Phys. JETP **56**, (1982)].
[2]E. K. Storm, H. F. Ahlstrom, M. J. Boyle, *et al.*, Phys. Rev. Lett. **40**, 1570 (1970).
[3]F. M. Abzaev, N. N. Beznasyuk, V. G. Bezuglov, *et al.*, Zh. Eksp. Teor. Fiz. **82**, 459 (1982) [Sov. Phys. JETP **55**, 263 (1982)].
[4]K. A. Brueckner and S. Jorna, Controlled Nuclear Fusion [Russ. transl.], Atomizdat, 1977, p. 8.
[5]S. Jackel, J. Albritton, and E. Foldman, Phys. Rev. Lett. **35**, 514 (1975); **37**, 95 (1976).
[6]Yu. A. Zakharenkov, A. A. Kologrivov, G. V. Sklizkov, and A. S. Shikanov, FIAN Preprint No. 74, 1977.
[7]N. G. Basov, A. A. Erokhin, Yu. A. Zakharenkov, *et al.*, Pis'ma Zh. Eksp. Teor. Fiz. **26**, 581 (1977) [JETP Lett. **26**, 433 (1977)].
[8]N. G. Basov, P. P. Volosevich, E. G. Gamaliĭ, *et al.*, Pis'ma Zh. Eksp. Teor. Fiz. **28**, 135 (1978) [JETP Lett. **28**, 125 (1978)].
[9]R. A. Haas, H. D. Shay, W. L. Kruer, *et al.*, Phys. Rev. Lett. **39**, 1533 (1977).
[10]H. D. Shay, R. A. Haas, W. L. Kruer, *et al.*, Phys. Fluids, **21**, 1634 (1978)
[11]K. Brueckner, R. Cover, R. Janda, *et al.*, Freprint KMSF, V-176, 1975.
[12]M. Lubin, E. Foldman, J. Soures, *et al.*, Proc. Fuj. Seminar Laser Interaction Plasma, 1975.
[13]V. L. Ginzburg, Rasprostranenie elektromagnitnykh voln v plazme (Propagation of Electromagnetic Waves in Plasma), Fizmatgiz, 1960, p. 278 [Gordon & Breach, 1961].
[14]K. Brueckner and R. Janada, Nuclear Fusion **17**, 451 (1977).
[15]C. E. Mac and C. F. McKee, Phys. Rev. Lett. **39**, 1336 (1977).
[16]J. Virmont, R. Pellat, and A. Mora, Phys. Fluids **21**, 567 (1978).
[17]D. T. Atwood, D. W. Sweeney, J. M. Auerbach, and P. H. Y. Lee, Phys. Rev. Lett. **40**, 184 (1978).
[18]L. Spitzer, Physics of Fully Ionized Gases, Wiley, 1962. Russ. transl. of earlier ed., IIL, 1957, p. 192.
[19]Yu. V. Afanas'ev, N. G. Basov, O. N. Krokhin, *et al.*, Interaction of High-Power Laser Radiation with Plasma, Itogi nauki i tekhniki (Sciences and Engineering Summaries), VINITI, Vol. 17, 1978.
[20]N. G. Denisov, Zh. Eksp. Teor. Fiz. **31**, 609 (1956) [Sov. Phys. JETP **4**, 544 (1957)].
[21]V. P. Silin, Pis'ma Zh. Eksp. Teor. Fiz. **21**, 333 (1975) [JETP Lett. **21**, 152 (1975)].
[22]E. Valeo, W. Kruer, V. Ruppert *et al.*, VCRL Preprint 78005, 1976.
[23]R. Hammerling, Plasma Physics **19**, 669 (1977).
[24]K. Brueckner, Phys. Rev. Lett. **36**, 677 (1976); **37**, 1247 (1976).
[25]K. Brueckner, Nuclear Fusion **17**, 1257 (1977).
[26]A. A. Erokhin S. A. Zverev, A. A. Kologrivov, *et al.*, Kratk. Soobshch. po Fiz. No. 9, 27 (1979).
[27]N. G. Basov, V. A. Boĭko, O. N. Krokhin, *et al.* Pis'ma Zh. Eksp. Teor. Fiz. **18**, 314 (1973) [JETP Lett. **18**, 184 (1973)].
[28]G. H. McCall, F. Yung, and G. Ehler, Phys. Rev. Lett. **30**, 1116 (1973).
[29]Yu. A. Sakharenkov, O. N. Krokin, G. V. Sklizkov, and A. S. Shikanov, Pis'ma Zh. Eksp. Teor. Fiz. **25**, 415 (1977) [JETP Lett. **25**, 388 (1977)].
[30]H. Azechi, Y. Sakagami, T. Yamanaka, and C. Yamanaka, Appl. Phys. Lett. **30**, 187 (1979).
[31]N. E. Andreev, Yu. A. Zakharenkov, and N. N. Zorev, Zh. Eksp. Teor. Fiz. **76**, 976 (1979) [Sov. Phys. JETP **49**, 492 (1979)].
[32]O. G. Baĭkov, V. I. Bayanov, A. A. Mak, *et al.*, Pis'ma Zh. Eksp. Teor. Fiz. **29**, 44 (1979) [JETP Lett. **29**, 40 (1979)].
[33]A. S. Ganeev, A. L. Zapysov, A. I. Zuev, *et al.*, Kvant. Elektron. (Moscow) **9**, 711 (1982) [Sov. J. Quantum Electron. **12**, 439 (1982)].
[34]G. N. Vinokurov, A. A. Mak, and V. A. Serebryakov, Kvant. Elektron. (Moscow) **3**, 1591 (1976) [Sov. J. Quantum Electron. **6**, 861 (1976).
[35]A. E. Danilov, N. N. Demchenko. V. B. Rozanov, G. V. Sklizkov, and S. I. Fedotov, Kvant. Elektron. (Moscow) **4**, 1034 (1977) [Sov. J. Quantum Elektron. **7**, 579 (1977)].
[36]V. V. Volenko and B. V. Kryuchenkov, Kvant. Elektron. (Moscow) **6**, 1343 (1979) [Sov. J. Quantum Electron. **9**, 789 (1979)].

Translated by J. G. Adashko